STABILISATION OF SAWTOOTH OSCILLATIONS BY LOWER HYBRID WAVES IN ASDEX

F. X. Söldner, D. Eckhartt, F. Leuterer, K. McCormick, G. Becker, H. S. Bosch, H. Brocken, H. Derfler, A. Eberhagen, G. Fussmann, O. Gehre, J. Gernhardt, G.v.Gierke, E. Glock, O. Gruber, G. Haas, J. Hofmann, A. Izvozchikov[1], G. Janeschitz, F. Karger, M. Keilhacker[2], O. Klüber, M. Kornherr, K. Lackner, M. Lenoci, G. Lisitano, F. Mast, H. M. Mayer, D. Meisel, V. Mertens, E. R. Müller[2], M. Münich, H. Murmann, H. Niedermeyer, A. Pietrzyk[3], W. Poschenrieder, H. Rapp, H. Riedler, H. Röhr, J. Roth, F. Ryter[4], F. Schneider, C. Setzensack, G. Siller, P. Smeulders[2], E. Speth, K.-H. Steuer, T. Vien, O. Vollmer, F. Wagner, D. Zasche, M. Zouhar

Max-Planck-Institut für Plasmaphysik
EURATOM Association, D-8046 Garching

Introduction:

Stabilisation of sawteeth has become a clue problem for high power additional heating in large tokamaks where the oscillations in the central electron temperature may be as high as 50 % /1/. In Lower Hybrid experiments the sawteeth of Ohmic discharges have been observed to disappear /2/, /3/. In this paper we study the parameter range for stabilisation of sawteeth accessible with the LH-system on ASDEX /4/, /5/. The role of the LH wave spectrum is discussed. For application to NBI heating the LH-power requirements and the benefits for the energy confinement in sawtooth-free discharges are investigated.

Stabilisation of sawteeth in OH-discharges

The sawtooth period τ_{st} rises upon injection of LH waves in a density range where the waves couple to suprathermal electrons ($\bar{n}_e \lesssim 3 \times 10^{13} cm^{-3}$). In the case of LH-current drive τ_{st} continues to change during the rf pulse. The values for the first sawtooth after start of the LH and for the saturated state are shown in Fig. 1 for a power scan at $\bar{n}_e = 1.6 \times 10^{13}$ cm^{-3}. At low power the sawtooth period rises continuously until the end of the rf. For $P_{LH} > 400$ kW τ_{st} first increases and then decreases, at high rf power even below the Ohmic value. Above a threshold P_{LH}^* the sawteeth finally disappear. The time delay τ_d between start of the LH and the last sawtooth collapse depends strongly on the density and it decreases with increasing rf power as shown in Fig. 2. The threshold P_{LH}^* there is marked by dashed lines. Stabilisation of sawteeth is possible only by applying LH-current drive spectra. With symmetric spectra in the LH-heating mode the sawtooth period may be changed but sawteeth remain present during the whole LH pulse ($\tau \le 1.5$ s) even at rf powers more than a factor of 2 above the threshold P_{LH}^* with LH-current drive.

The mechanism for sawtooth stabilisation might therefore be seeked in the change of the current profile j(r) connected with LH current drive. The internal inductance l_i may be derived from magnetic measurements with some precautions. From the quantities $\beta_p^{equ} + l_i/2$ (derived from the equilibrium fields) and $\beta_p^{\perp}$ (from diamagnetic measurements) l_i can only be determined if

[1]Academy of Sciences, Leningrad, USSR; [2]Present address: JET Joint Undertaking, England; [3]Univ. of Washington, Seattle USA; [5]CEN Grenoble, France

the pressure is isotropic. During heating and current drive with LH waves of high phase velocity ($\bar{v}_{ph,\parallel} = c/2$), however, the pressure may become highly anisotropic due to the generation of fast electrons parallel to the magnetic field /7/. Therefore direct measurements of j(r) were made for various modes of LH operation in ASDEX /8/, /9/. In the case of the LH power scan at $\bar{n}_e = 1.6 \times 10^{13}\ cm^{-3}$ (Figs. 1,2) the pressure anisotropy remains small and the stationary value of $(\beta_p^{equ} + l_i/2) - \beta_p^{\perp}$ then gives l_i. At low rf power l_i increases while it drops during LH current drive with $P_{LH} > 400$ kW as seen from Fig. 3. Consequently, the current profile is peaking during low power LH-current drive and the higher increase of the sawtooth period τ_{st} in Fig. 1 might then be explained by an expansion of the sawtooth-unstable region within r(q=1). The drop in l_i at higher power indicates a flattening of j(r) and the reduction in τ_{st} could be explained in like manner by a shrinking of the q=1-surface. With $P_{LH} > P_{LH}^*$ j(r) flattens to such an extent that the q=1 surface disappears and q > 1 in the entire plasma region /9/. Stabilisation of the sawteeth is therefore achieved if j(r) is modified such that the instability condition (q=1 at some radius) is removed. On ASDEX, so far, this is the only method how sawteeth could be suppressed by means of LH waves.

In the parameter range where sawteeth were stabilized about half of the rf power necessary for complete LH-current drive was required. For discharges with q(a) = 3.5 this can be seen from Fig. 4 where the relative reduction in Ohmic input $-\Delta P_{OH}^*/P_{OH}$ due to LH current drive at the stability margin with $P_{LH} = P_{LH}^*$ is plotted versus $\bar{n}_e$ together with the absorbable fraction $P_{LH,acc}^*$ of the rf power launched in these cases. Because of the uncertainty in the deposition profile two cases have been considered for accessibility to a/3 and 2a/3 /7/.

Stabilisation of sawteeth during NBI:

The sawtooth period τ_{st} during NBI increases with increasing beam power P_{NI} (Fig. 5) and above a certain threshold in P_{NI} which augments with $\bar{n}_e$ no sawteeth are observed during NBI. In sawtoothing discharges with NBI τ_{st} rises upon injection of LH power both in heating and current drive mode. Suppression of sawteeth is possible with LH current drive only. The mechanism of stabilisation is again related to a flattening of the current profile j(r) as indicated by a decrease of l_i. The drop in l_i does not depend on P_{NI} but only on P_{LH} and on the wave spectrum. The minimum rf power required for stabilisation P_{LH}^* is reduced for higher P_{NI} as seen from Fig. 5.

This suggests that the current profile is flattened in the central plasma region already by NBI alone and less LH-power is therefore required for higher P_{NI} to remove the q=1 surface from the plasma.

With counter-NBI the threshold power P_{LH}^* is even further reduced as seen in Fig. 5. Also with NBI alone sawteeth disappear already at lower power in this case. This seems to be mainly due to the broad $T_e(r)$ profiles which are observed with counter-NBI. The shorter sawtooth period (Fig. 5) might be also explained by this fact. A contribution from a counter-driven beam current reducing the net plasma current in the center and thereby flattening j(r) as proposed in a scenario for sawtooth suppression /10/ cannot be ruled out.

In sawtooth-free discharges with NBI higher central electron temperatures can be obtained. The $T_e(r)$ profiles are plotted in Fig. 6 for the Ohmic phase, NBI alone and for NBI combined with LH current drive. With P_{LH} = 540 kW which is below P_{LH}^* the $T_e(r)$ profiles still resemble the profiles with NBI alone. The additional LH power replaces mainly the drop in P_{OH} in this case. With $P_{LH} > P_{LH}^*$ (P_{LH} = 720 kW) sawteeth are suppressed and the central temperatures increase. The resulting increase in total energy content is small because of the small volume where sawteeth dominate the power loss. With lower q(a) the sawtooth-unstable region is larger and a larger gain for global plasma heating can be obtained. At q(a) = 2.75 (I_p = 380 kA, B_t = 2.2 T) sawtooth suppression with P_{LH} = 550 kW resulted in a 30 % increase of the total plasma energy content from NBI with P_{NI} = 1.8 MW. Improvement of the central confinement by stabilisation of the sawteeth therefore contributes also to an appreciable improvement of the global confinement.

References
/1/ J. Jacquinot, et al., Plasma Physics and Controlled Fus. 28, 1 (1986).
/2/ J.E. Stevens, R. Bell, S. Bernabei, et al., 12th Europ. Conf. on Contr. Fusion and Plasma Physics, Budapest, 1985, Vol. II, p. 192.
/3/ F. Parlange, et al., in Ref. /2/, Vol. II, p. 172.
/4/ D. Eckhartt, et al., 4th Int. Symposium on Heating in Toroidal Plasmas, Rome, 1984, Vol. I, p. 501.
/5/ F. Leuterer, F. Söldner, D. Eckhartt, et al., Plasma Physics and Controlled Fusion 27, 1399 (1985).
/6/ F. Leuterer, D. Eckhartt, F. Söldner, et al., in Ref. /2/, Vol. II, p. 240.
/7/ F. Söldner, D. Eckhartt, F. Leuterer, et al., in Ref. /2/, Vol. II, p. 244.
/8/ K. McCormick, et al., in Ref. /2/, Vol. I, p. 199.
/9/ K. McCormick, et al., this conference.
/10/ J. Jacquinot, private communication.

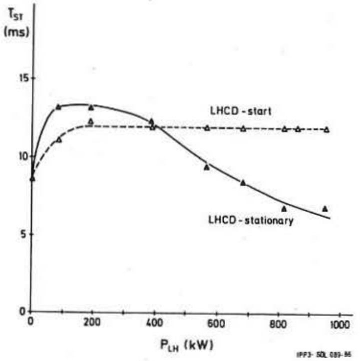

Fig. 1: Sawtooth period τ_{st} during LH-current drive versus LH-power.

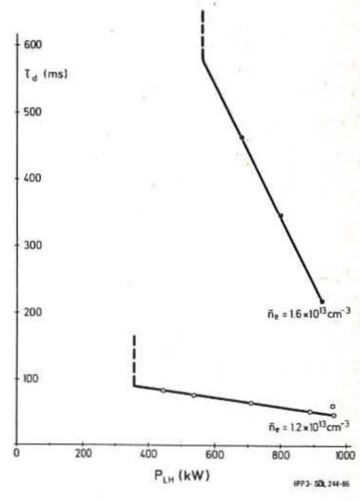

Fig. 2: Time delay τ_d for sawtooth suppression after start of LH versus LH-power.

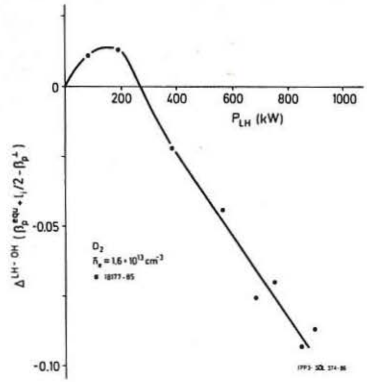

Fig. 3: Variation of the quantity $(\beta_p^{equ} + l_i/2) - \beta_p^{\perp}$ with P_{LH} during LH-current drive.

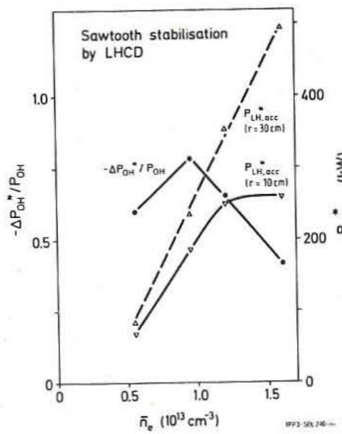

Fig. 4: Drop in ohmic power $-\Delta P_{OH}^*/P_{OH}$ and accessible fraction of LH-power $P^*_{LH,acc}$ at the margin for sawtooth stabilization $P_{LH} = P_{LH}^*$ as function of $\bar{n}_e$.

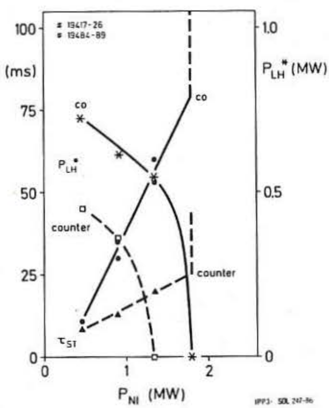

Fig. 5: Sawtooth period τ_{st} for NBI and threshold power P_{LH}^* for sawtooth stabilization by LH during NBI for co- and counter-injection as function of P_{NI}.

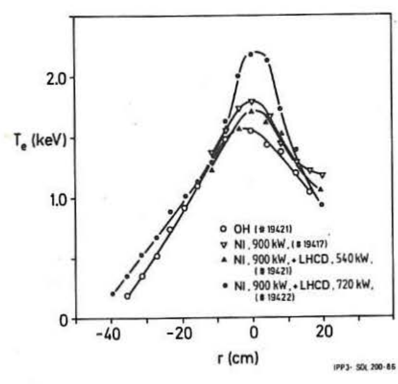

Fig. 6: $T_e(r)$ profiles during OH- and NBI-heating and for the sawtooth-free phase of NBI + LHCD (P_{LH} = 720 kW).